

Synthesis, structure, and properties of the high-temperature superconductor $\text{HgBa}_2\text{CuO}_{4+\delta}$

J. P. Hodges, I. Gameson, and P. P. Edwards*

School of Chemistry, The University of Birmingham, Edgbaston, Birmingham, B15 2TT, United Kingdom

A. P. Kharel and A. Porch

School of Electrical Engineering, The University of Birmingham, Edgbaston, Birmingham, B15 2TT, United Kingdom

(Received 18 November 1996)

We report here the attempted synthesis of $(\text{Hg}_{1-x}\text{Cu}_y)\text{Ba}_2\text{CuO}_{4+\delta}$ ($0 \leq x \leq 0.2$, $0 \leq y \leq 0.2$, $y \leq x$) and the results of a detailed characterization of the structural and superconducting properties of the resulting samples. Rietveld refinement of powder x-ray-diffraction data collected on all 15 samples synthesized found no partial Cu occupancy of the Hg site. We therefore conclude that for these samples no solid solution exists and the superconducting phase is simply $\text{HgBa}_2\text{CuO}_{4+\delta}$. Only one interstitial oxygen position O(3) was found, located exactly at the center of the Hg plane. An analysis of the structural refinements has produced a number of correlations between the exact location of the Ba^{2+} cation within the unit cell and a number of important superconducting parameters; these include the occupancy of the O(3) site, the extent of oxidation of the CuO_2 planes, and the magnetic penetration depth. [S0163-1829(97)09517-9]

I. INTRODUCTION

In 1991, Putlin, Bryntse, and Antipov¹ reported the synthesis of layered cuprates containing discrete (HgO_δ) layers, $\text{HgBa}_2\text{RCu}_2\text{O}_{6+\delta}$. Unfortunately, in spite of their obvious structural similarity with $\text{TlBa}_2\text{CaCu}_2\text{O}_{7+\delta}$ ($T_c = 85$ K), no superconductivity was detected in these cuprates. Subsequently, the Hg-layered cuprate superconductor $\text{HgBa}_2\text{CuO}_{4+\delta}$ (Hg1201) with a $T_c = 94$ K was reported in 1993.²

Hg1201 is the first member of the homologous series $\text{HgBa}_2\text{Ca}_{n-1}\text{Cu}_n\text{O}_{2n+2+\delta}$, with $n \geq 1$. The discovery of the two superconducting higher homologues, $\text{HgBa}_2\text{CaCu}_2\text{O}_{6+\delta}$ (Hg1212) and $\text{HgBa}_2\text{Ca}_2\text{Cu}_3\text{O}_{8+\delta}$ (Hg1223) (Ref. 3) with $T_c = 128$ and 135 K, respectively, swiftly followed that of Hg1201. The basic crystal structure of these three compounds has been revealed by a number of powder neutron-diffraction studies,⁴⁻⁸ and it is widely agreed that the structures contain the following layer sequence:

$$\dots[(\text{BaO})_c(\text{HgO}_\delta)_o(\text{BaO})_c(\text{CuO}_2)_o(n-1) \\ \times \{(\text{Ca})_c(\text{CuO}_2)_o\}] \dots,$$

where the subscripts c and o indicate whether the cation is at the center or origin of the mesh for each layer. A schematic representation of the crystal structure of Hg1201 is presented in Fig. 1. There exists however, a degree of controversy regarding the precise structure/composition of the (HgO_δ) layer. Diffraction studies have revealed the presence of an interstitial oxygen defect located at or close to the $(1/2, 1/2, 0)$ site in the center of the Hg plane. Furthermore, Wagner *et al.* found an additional defect involving partial substitution of Hg by Cu coupled to the presence of oxygen at the $(1/2, 0, 0)$ site.⁴ These authors determined that Cu had substituted for 7(1)% of the Hg in Hg1201 and therefore the actual stoichiometry of the Hg1201 superconductor is better represented by $(\text{Hg}_{0.93}\text{Cu}_{0.07})\text{Ba}_2\text{CuO}_{4+\delta}$. Recent detailed structural stud-

ies performed on Hg1201,⁹ and the higher homologues Hg1212 and Hg1223,^{10,11} have provided additional evidence for the existence of this coupled Cu-O defect.

If Cu is partially substituting for Hg in the Hg-layered superconductors, then there should exist a solid-solution of the form $(\text{Hg}_{1-y}\text{Cu}_y)\text{Ba}_2\text{CuO}_{4+\delta}$. There is another possibility, however, a solid-solution field of the form $(\text{Hg}_{1-x}\text{Cu}_y)\text{Ba}_2\text{CuO}_{4+\delta}$ which incorporates both Cu partially substituting for Hg and Hg vacant sites (i.e., when $x > y$) may exist. Here the solid-solution line $(\text{Hg}_{1-y}\text{Cu}_y)\text{Ba}_2\text{CuO}_{4+\delta}$ is the edge of the solid-solution field $(\text{Hg}_{1-x}\text{Cu}_y)\text{Ba}_2\text{CuO}_{4+\delta}$ where $x = y$. In order to verify the existence of such a solid-solution field or line, we have studied the effect of nominal starting composition upon the synthesis, crystal structure, and superconducting properties of Hg1201. In an effort to increase our understanding of the origin of superconductivity in Hg1201, we have also investigated the relationships between crystal structure and superconducting properties.

II. EXPERIMENT

A. Synthesis of samples

A precursor, $\text{Ba}_2\text{CuO}_{3.3}$, was obtained by solid-state reaction of a stoichiometric mixture of BaO and CuO in flowing O_2 gas at 930 °C for 45 h, followed by a slow cool at 40 °C h⁻¹, with two intermittent grindings. Since $\text{Ba}_2\text{CuO}_{3.3}$ is susceptible to degradation from atmospheric moisture and CO_2 this precursor was immediately transferred to an argon glovebox (2–10 ppm H_2O , 5–40 ppm O_2).

Polycrystalline samples with nominal starting compositions $(\text{Hg}_{1-x}\text{Cu}_y)\text{Ba}_2\text{CuO}_{4+\delta}$ ($y \leq x$, y and $x = 0.00, 0.05, 0.10, 0.15, 0.20, 15$ samples in total) were prepared as follows. Appropriate amounts of $\text{Ba}_2\text{CuO}_{3.3}$ and CuO were intimately mixed with 1.4 mmol of HgO (~ 0.3 g), compacted into pellets and wrapped in Ag foil, all within a glovebox. These pelletized samples were then individually sealed in quartz tubes (I.D. 13 mm, O.D. 16 mm, length ~ 100 mm)

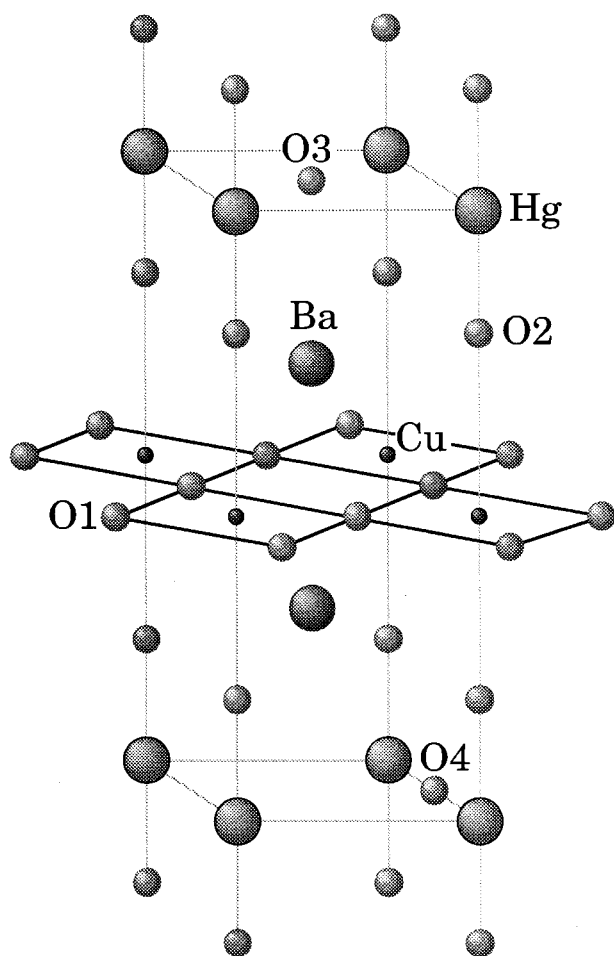


FIG. 1. A schematic representation of the structure of $\text{HgBa}_2\text{CuO}_{4+\delta}$.

containing air at 1 atm pressure and placed in steel containers. These were then heated to 800 °C in 4 h, held at 800 °C for 8 h, and finally slowly cooled to room temperature over a period of 8 h.

B. Powder x-ray-diffraction and data analysis

Powder x-ray-diffraction data were collected in transmission mode using a Siemens D5000 x-ray diffractometer ($\text{Cu } K\alpha_1$ radiation, $\lambda = 1.5406 \text{ \AA}$) fitted with a position sensitive detector. Structural refinements were performed by the Rietveld method,¹² assuming neutral atom x-ray form factors, using the GSAS suite of programs.¹³ The step-scan diffraction data were collected on as-synthesized samples over the angular range $10^\circ \leq 2\theta \leq 100^\circ$. A 2θ step size of 0.02° and a counting time of 10 s per data point were used. No evidence of preferred orientation was found in any of the data sets collected.

C. ac susceptibility measurements

The ac susceptibility measurements were performed on finely powdered samples in a nominally zero dc field, using a frequency of 1 kHz in the 10–200 K temperature range. Superconducting transition temperatures were determined from

the real part decrease of the magnetic susceptibility, χ . A mean density of 5 g cm^{-3} was determined for the sintered barlike samples, $\sim 70\%$ of the theoretical density ($\rho = 7.05 \text{ g cm}^{-3}$). Apparent superconducting volume fractions (no correction was applied for demagnetization and size effects) were calculated from the magnetic susceptibilities measured at a temperature of 10 K.¹⁴

D. Magnetic penetration depth measurements

The microwave measurement of the magnetic penetration depth, λ , was performed using a cavity perturbation technique designed specifically for measurements on powder samples of high-temperature superconductors.¹⁵ This technique involves placing the sample in the microwave magnetic field of a quarter wave copper hairpin resonator ($\nu_{\text{res}} = 4.2 \text{ GHz}$). The powder grains were diluted in a low loss, low melting point wax (Okerin) to minimize the effects of intergrain contacts. The screening currents induced in each grain in the superconducting state results in a decrease of the resonant frequency of the stripline. Consequently, measurements of the resonant frequency shift can be used to determine absolute values of λ , where we use a model of isolated spherical grains and a grain-size distribution determined from high-resolution SEM photographs (JEOL 5200) of the powder samples. The errors in the values of λ are relatively unaffected by variation in grain shape, but are more sensitive to uncertainties in the powder grain-size distribution. For this reason, the absolute values of λ are in error by $\sim \pm 0.2 \text{ }\mu\text{m}$.

III. RESULTS AND DISCUSSION

A. Unit-cell parameters

For all 15 samples prepared, of nominal starting compositions $(\text{Hg}_{1-x}\text{Cu}_y)\text{Ba}_2\text{CuO}_{4+\delta}$ ($y \leq x, y$ and $x = 0.00, 0.05, 0.10, 0.15, 0.20$) referred to as Hg(00)–Hg(44), Table I lists the nominal starting composition variables x and y , refined unit-cell parameters and the superconducting parameters, T_c and the measured magnetic susceptibility at a temperature of 10 K.

The unit-cell parameters obtained are consistent with previously reported values for Hg1201 synthesized by the sealed quartz tube technique.^{2,4,9} With regard to the existence of a solid-solution line, $(\text{Hg}_{1-y}\text{Cu}_y)\text{Ba}_2\text{CuO}_{4+\delta}$, or a solid-solution field, $(\text{Hg}_{1-x}\text{Cu}_y)\text{Ba}_2\text{CuO}_{4+\delta}$, it could be anticipated that the unit-cell parameters would display a simple dependence with the initial composition variables, x and y . Examination of Table I, however, shows that no such simple relationship exists between the nominal composition variables and the unit-cell parameters of the subsequently synthesized materials. The observation of such a correlation would be considered as positive evidence for the existence of a solid solution. However, the absence of a correlation does not inviolate this proposal, since other factors, most notably oxygen content, may be critical in determining the unit-cell parameters.

B. Superconducting properties

The effect of nominal starting composition upon the superconducting properties of the resulting materials has been

TABLE I. The refined unit-cell dimensions and superconducting parameters of samples synthesized from pellets of nominal starting composition $(\text{Hg}_{1-x}\text{Cu}_y)\text{Ba}_2\text{CuO}_{4+\delta}$

Sample	x	y	a (Å)	c (Å)	T_c (K) ^a	χ at 10 K (emu g ⁻¹)
Hg(00)	0.00	0.00	3.871(3)	9.493(3)	91.0	-0.0055
Hg(10)	0.05	0.00	3.868(3)	9.484(3)	89.5	-0.0070
Hg(11)	0.05	0.05	3.873(3)	9.494(3)	95.2	-0.0099
Hg(20)	0.10	0.00	3.876(3)	9.502(3)	96.0	-0.0085
Hg(21)	0.10	0.05	3.872(3)	9.496(3)	96.0	-0.0111
Hg(22)	0.10	0.10	3.874(3)	9.499(3)	95.3	-0.0136
Hg(30)	0.15	0.00	3.870(3)	9.492(3)	93.0	-0.0075
Hg(31)	0.15	0.05	3.872(3)	9.497(3)	95.5	-0.0102
Hg(32)	0.15	0.10	3.874(3)	9.497(3)	94.5	-0.0121
Hg(33)	0.15	0.15	3.872(3)	9.495(3)	95.5	-0.0115
Hg(40)	0.20	0.00	3.873(3)	9.499(3)	94.5	-0.0071
Hg(41)	0.20	0.05	3.870(3)	9.492(3)	95.8	-0.0104
Hg(42)	0.20	0.10	3.872(3)	9.494(3)	94.3	-0.0110
Hg(43)	0.20	0.15	3.875(3)	9.502(3)	93.2	-0.0114
Hg(44)	0.20	0.20	3.870(3)	9.490(3)	95.4	-0.0084

^aEstimated error on T_c is ± 0.5 K.

studied. The majority of as-synthesized samples displayed T_c 's within 3 K of the optimum value of 96 K. No obvious relationship could be discerned between the measured T_c 's and nominal starting compositions. Figure 2 presents the ac susceptibility data for the samples Hg(00), Hg(11), Hg(22), Hg(33), and Hg(44), i.e., for the solid-solution line $(\text{Hg}_{1-y}\text{Cu}_y)\text{Ba}_2\text{CuO}_{4+\delta}$. Clearly, for these particular samples, the apparent superconducting volume fraction, V_F , determined from the magnetic susceptibility at 10 K, varies significantly between samples whereas, T_c appears to be relatively independent. The apparent superconducting volume fractions for all the samples synthesized were found to vary between 30 and 85 %.

The superconducting properties of Hg1201 are examined in further detail in Sec. III D. In particular, the bulk superconducting properties of Hg1201 are shown to be related to subtle variations in crystal structure.

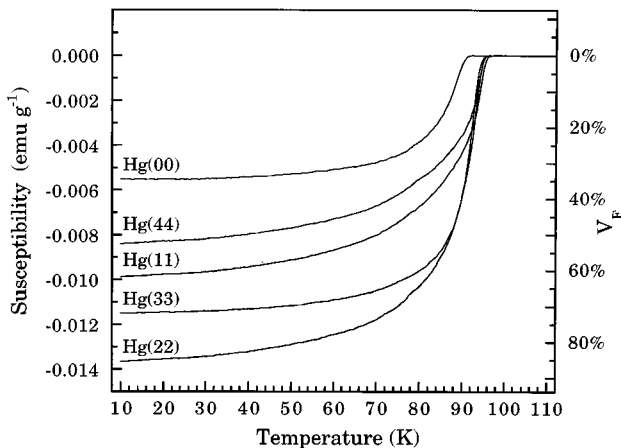


FIG. 2. Magnetic susceptibility for samples of nominal starting composition $(\text{Hg}_{1-y}\text{Cu}_y)\text{Ba}_2\text{CuO}_{4+\delta}$ ($y = 0.0, 0.05, 0.10, 0.15$, and 0.20).

C. Crystal structure refinements

Powder x-ray diffraction showed that all but one of the samples synthesized were of high purity ($> 90\%$). Sample Hg(00) of nominal starting stoichiometry $\text{HgBa}_2\text{CuO}_{4+\delta}$ was found to contain a significant amount of impurity phases ($> 10\%$)—these include $\text{Ba}_2\text{Cu}_3\text{O}_{5+\delta}$, BaHgO_2 , $\text{Ba}_2\text{CuO}_{3.3}$, and CuO . The powder x-ray-diffraction profiles obtained from samples Hg(00) and Hg(11) are presented in Fig. 3.

This observation alone is particularly interesting; the use of a reaction mixture of nominal composition

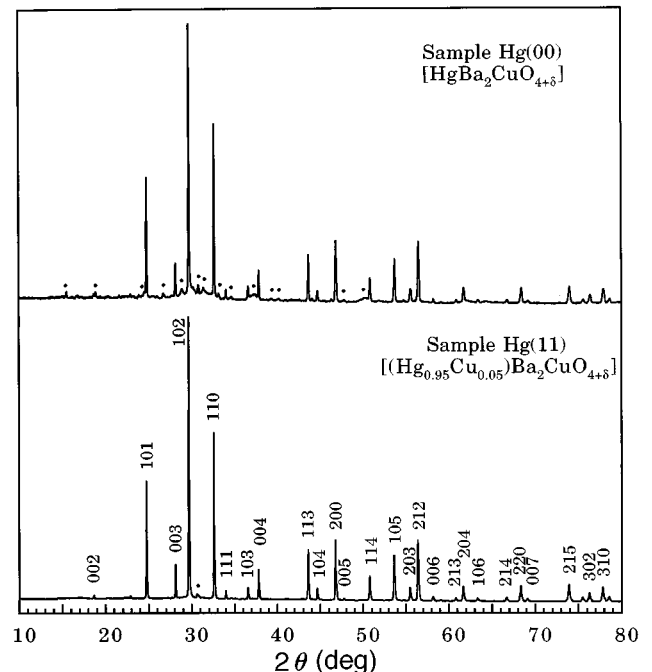


FIG. 3. The powder x-ray-diffraction profiles of samples Hg(00) and Hg(11). The dots mark peaks resulting from the presence of various impurity phases.

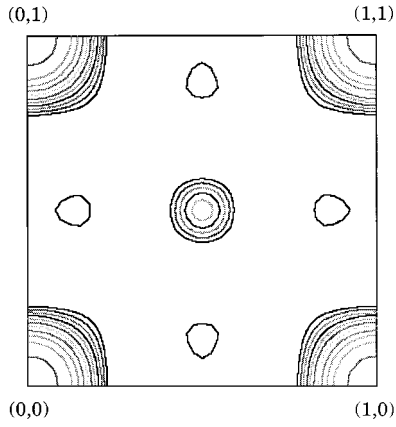


FIG. 4. The difference electron-density map for the $(xy0)$ section of Hg1201 [sample Hg(20), of nominal starting composition $\text{Hg}_{0.9}\text{Ba}_2\text{CuO}_{4+\delta}$]. Contour level is set at 0.2% of $F_{\text{obs}}(\text{Hg})$.

$\text{HgBa}_2\text{CuO}_{4+\delta}$ results in the production of impure Hg1201 under the normal synthesis conditions outlined in Sec. II A. This is consistent with the difficulties encountered by many groups in preparing monophasic Hg1201. Recently however, two modified synthesis routes, the first involving a rapid-heat rapid-cool technique⁹ and the second using mixtures of transition-metal oxides to regulate partial oxygen pressure,¹⁶ have successfully prepared monophasic Hg1201 from a stoichiometric reaction mixture.

Structural refinements were performed by the Rietveld method. The tetragonal space group $P4/mmm$ reported in previous studies of Hg1201 was assumed and the initial atom positions were those reported by Putlin *et al.*² The initial refinements were based on a model that excluded the partially occupied O(3) oxygen site at $(1/2, 1/2, 0)$. All positional variables and isotropic thermal parameters were refined. Regions containing minor peaks originating from secondary phases were excluded from the refinements. Typically a small amount of $\text{Ba}_2\text{CuO}_{3.3}$ was detected in all the

powder x-ray-diffraction profiles. Difference Fourier methods were then used to locate any partial oxygen sites within the Hg layer.

Refinement of the simple structural model of $\text{HgBa}_2\text{CuO}_4$ converged to give a satisfactory fit to the data for all the samples. The position of a single additional oxygen site was located in the Hg layer by analysis of difference Fourier maps of the (001) plane. These difference maps revealed the presence of a prominent maximum located at $(1/2, 1/2, 0)$, which corresponds to the proposed O(3) oxygen site. The Fourier section obtained from sample Hg(20) is presented in Fig. 4. The Fourier maps showed no significant electron density at the site $(1/2, 0, 0)$, corresponding to the proposed O(4) partial oxygen site,^{4,9-11} nor did they suggest any static displacement of the O(3) site away from the center position.^{9,10}

The inclusion of the additional O(3) oxygen site in the refinements (occupancy being refined from an initial value of 0.10) yielded lower residual factors (R_{wp}, R_p). The isotropic thermal parameter of the partially occupied O(3) site was fixed at a value of $B_{\text{iso}} = 1.5 \text{ \AA}^2$. Refined values of the O(3) site occupancy were found to vary between 0.07 and 0.25, with the majority in the range 0.09 to 0.15. Considering the relative X-ray-scattering powers of both oxygen and Hg atoms, it is unreasonable to expect a greater degree of precision in measuring the occupancy of the O(3) site. The final refined parameters for all 15 samples are presented in Table II.

D. Structural relationships in Hg1201

It may, however, be possible to estimate the occupancy of the O(3) site indirectly. It is widely believed that the occupancy of the O(3) site results in an injection of holes into the CuO_2 planes leading to superconductivity.¹⁷ The position of the Ba atom within the unit cell is largely determined by electrostatic forces, and therefore is influenced by the number of charge carriers present within the CuO_2 planes. Since oppositely charged ions are attracted to one another, an in-

TABLE II. Final refined structural parameters and Cu bond-valence sums (BVS) for all 15 samples of Hg1201 synthesized. $R_{wp} = [\{\sum_i w_i |y_i(\text{obs}) - y_i(\text{calc})|^2\} / \{\sum_i w_i y_i^2(\text{obs})\}]^{1/2}$, $R_p = [\{\sum_i |y_i(\text{obs}) - y_i(\text{calc})|^2\} / \{\sum_i y_i^2(\text{obs})\}]^{1/2}$, $R_e = [N - P + C / \sum_i w_i y_i^2(\text{obs})]^{1/2}$, $R_I = [\sum_k |I_k(\text{obs}) - (1/c)I_k(\text{calc})| / \sum_k I_k(\text{obs})]$, where N , P , and C are the number of observations, parameters, and constraints, respectively.

Sample	Hg(00)	Hg(10)	Hg(11)	Hg(20)	Hg(21)	Hg(22)	Hg(30)	Hg(31)	Hg(32)	Hg(33)	Hg(40)	Hg(41)	Hg(42)	Hg(43)	Hg(44)	esd
Hg Occ	1.050	0.922	0.987	0.980	0.989	1.001	0.986	0.996	0.987	0.998	0.960	0.986	0.998	0.986	0.986	10
Hg B_{iso} (\AA^2)	1.9	2.4	2.3	2.5	2.5	2.7	2.3	2.1	2.7	2.5	2.4	2.7	2.7	2.8	2.6	1
Ba z (z_{Ba})	0.2970	0.2971	0.2986	0.2981	0.2981	0.2989	0.2978	0.2985	0.2987	0.2982	0.2978	0.2987	0.2990	0.2992	0.2982	1
Ba B_{iso} (\AA^2)	1.3	1.3	1.6	1.7	1.7	2.1	1.4	1.3	2.0	1.9	1.4	1.9	2.0	2.1	1.9	1
Cu B_{iso} (\AA^2)	0.6	0.7	1.1	1.2	1.3	1.7	1.2	0.7	1.6	1.6	1.1	1.5	1.7	1.8	1.5	1
O(1) B_{iso} (\AA^2)	1.4	0.6	0.4	1.2	0.9	1.3	1.0	0.3	1.5	1.2	0.8	1.4	1.6	2.0	1.7	3
O(2) _z	0.210	0.209	0.209	0.207	0.207	0.207	0.209	0.207	0.209	0.210	0.208	0.209	0.208	0.208	0.208	2
O(2) B_{iso} (\AA^2)	1.6	1.4	1.7	2.0	2.2	2.4	2.0	0.9	2.5	2.4	1.2	2.4	2.4	2.5	2.3	3
O(3) Occ	0.25	0.25	0.09	0.09	0.21	0.14	0.20	0.14	0.12	0.14	0.18	0.07	0.13	0.12	0.13	5
R_{wp}	5.9%	6.4%	6.7%	6.6%	5.7%	6.8%	4.7%	5.7%	6.1%	5.4%	5.3%	5.4%	5.9%	6.6%	5.4%	
R_p	4.5%	4.8%	4.8%	4.8%	4.1%	4.8%	3.5%	4.3%	4.5%	4.1%	4.0%	4.1%	4.4%	4.8%	3.9%	
R_e	2.3%	3.5%	2.2%	3.2%	2.7%	2.5%	2.5%	2.9%	2.6%	2.9%	2.7%	2.8%	3.1%	3.0%	2.5%	
R_I	11.3%	5.9%	5.0%	4.2%	5.2%	4.2%	5.7%	5.3%	4.8%	4.7%	4.8%	3.2%	5.2%	4.4%	7.4%	
BVS	2.16	2.17	2.14	2.13	2.14	2.14	2.16	2.14	2.14	2.15	2.14	2.16	2.15	2.14	2.15	

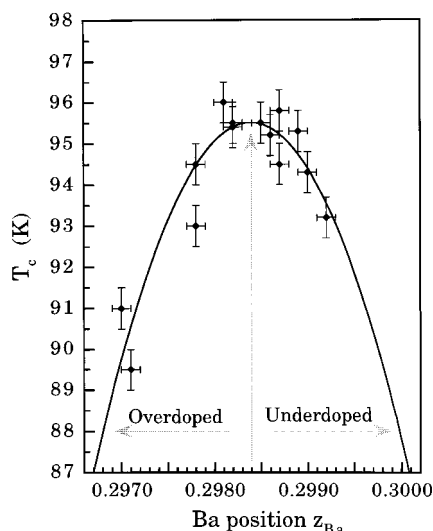


FIG. 5. Critical temperatures plotted as a function of the Ba atom z position parameter.

creased occupancy of the interstitial O(3) site would lead to a shorter Ba-O(3) bond. Consequently, a correlation between the Ba atom z position parameter, z_{Ba} , the occupancy of the O(3) site, and hence T_c may be anticipated. Figure 5 displays T_c as a function of z_{Ba} for all the samples synthesized. Clearly, there exists a quantitative relationship between z_{Ba} and T_c . The optimum position of the Ba atom within the unit cell is indicated in Fig. 5, i.e., $z_{\text{Ba}} = 0.2984(1)$. Furthermore, the conventional overdoped ($z_{\text{Ba}} < 0.2984$) and underdoped ($z_{\text{Ba}} > 0.2984$) regimes can be easily identified by such a curve.¹⁸

For powder x-ray-diffraction data, it is more difficult to delineate a precise relationship between O(3) occupancy and z_{Ba} . Accurate values for both O(3) occupancy and z_{Ba} have previously been determined by neutron powder-diffraction studies. Figure 6 presents reported values of O(3) occupancy as a function of z_{Ba} parameter. Since both Wagner *et al.*⁴ and

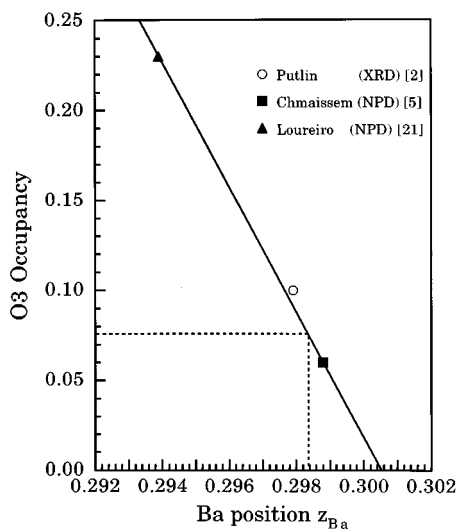


FIG. 6. Reported occupancies of the O(3) site plotted as a function of Ba atom z position parameter.

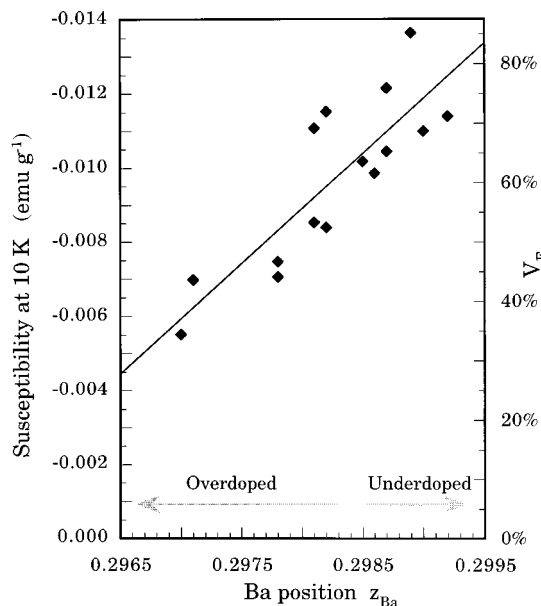


FIG. 7. Magnetic susceptibilities at 10 K plotted as a function of Ba atom z position parameter.

Asab *et al.*⁹ performed structural refinements of Hg1201 based on models that differed critically over the location and number of interstitial oxygen sites within the Hg layer, their respective data points were considered to be inappropriate for this discussion. If a linear relationship is assumed between O(3) occupancy and z_{Ba} , then the optimum O(3) occupancy is estimated to be 0.08(1). This value corresponds to a Cu valence of 2.16(2), widely considered to be the optimum value for superconductivity in cuprates.^{19,20} Figure 6 suggests that the range of O(3) occupancies for the samples synthesized, Hg(00)–Hg(44), is $0.05 \leq \delta \leq 0.13$. This range is in fair agreement with the range $0.09 \leq \delta \leq 0.18$ determined by Rietveld analysis of powder x-ray-diffraction data, see Table II. Cu bond-valence sums (BVS), based on a scheme proposed by Brown,²¹ calculated using the crystal data obtained from the 15 refinements, suggest an optimum Cu valence of 2.15(1), see Table II. This value is in excellent agreement with the independent value of 2.16(2), obtained from the estimated optimum occupancy of the O(3) site.

Interestingly z_{Ba} is not only correlated with the superconducting parameter T_c , but also with the apparent superconducting volume fraction, see Fig. 7. A general decrease in the apparent superconducting volume fraction is observed with increasing doping of CuO_2 planes. A similar correlation, between measured magnetic susceptibility and T_c , has recently been reported for a series of annealed Hg1201 samples.¹⁸ For the superconductors $\text{Tl}_2\text{Ba}_2\text{CuO}_{6+\delta}$ (Ref. 22) and $\text{TlBa}_2\text{CuO}_{5-\delta}$ (Ref. 23), it has been reported that $n_s/m^* \propto \lambda^{-2}$ decreases with increasing hole doping; here n_s is the superconducting carrier density and m^* is the effective mass. The low-field magnetization M of superconducting particles with diameter d is related¹⁸ to λ as $M \propto 1 - (\lambda/d)^2$. Therefore the observed correlation between measured magnetic susceptibility and z_{Ba} is a consequence of the magnetic penetration depth increasing with hole doping of the CuO_2 planes.

Magnetic penetration depth measurements were performed on samples Hg(00), Hg(22), and Hg(44), since these

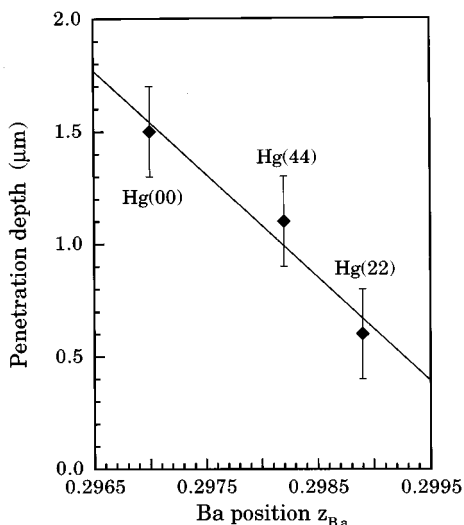


FIG. 8. Magnetic penetration depths for samples Hg(00), Hg(22), and Hg(44), of nominal starting compositions $\text{HgBa}_2\text{CuO}_{4+\delta}$, $(\text{Hg}_{0.9}\text{Cu}_{0.1})\text{Ba}_2\text{CuO}_{4+\delta}$ and $(\text{Hg}_{0.8}\text{Cu}_{0.2})\text{Ba}_2\text{CuO}_{4+\delta}$ plotted as a function of Ba atom z position parameter.

samples displayed a large variation in their apparent superconducting volume fractions and cover the range from overdoped through optimally doped to underdoped superconductors. As expected the measured magnetic penetration depths were found to correlate well with z_{Ba} , see Fig. 8 which shows a plot of λ versus z_{Ba} .

E. Defect structure

The possible substitution of Hg by either Cu or C in Hg1201 (a defect involving the incorporation CO_3^{2-} groups into the Hg layer has recently been proposed²⁴) was investigated by refining the occupancy of Hg at the (0,0,0) site. Figure 9 displays the refined Hg occupancies as a function of the nominal composition parameter y , the amount of Cu substitution expected if a solid solution of the form $(\text{Hg}_{1-x}\text{Cu}_y)\text{Ba}_2\text{CuO}_{4+\delta}$ exists. The results presented in Fig. 9 clearly show that the Hg occupancy is independent of y ; an occupancy of 0.99(1) for Hg has been determined from our measurements. Together these refinements strongly support the view that, for these samples, no defect involving the substitution of Hg by Cu is present within Hg1201 and its chemical formula is best represented as $\text{HgBa}_2\text{CuO}_{4+\delta}$. This is in contradiction to powder neutron-diffraction^{4,9,11} and related single-crystal x-ray-diffraction experiments.¹⁰ These results also preclude the incorporation of CO_3^{2-} groups within the Hg layer, since this would be detected in the same manner as Cu substitution, i.e., by a loss of scattering power from the Hg site. However, the possibility remains that CO_3^{2-} groups are substituting for Hg in samples of Hg1201 synthesized by the high-pressure technique.²⁴

The thermal parameters of Hg, Ba, Cu, O(1), and O(2), averaged over all 15 refinements, are presented in Table III. These thermal parameters are in agreement with those found previously by Putlin *et al.*² The thermal parameters of Hg and the coordinated O(2) ($B_{\text{iso}} \sim 2.2 \text{ \AA}^2$), were consistently found to be significantly higher than those of Cu and O(1)

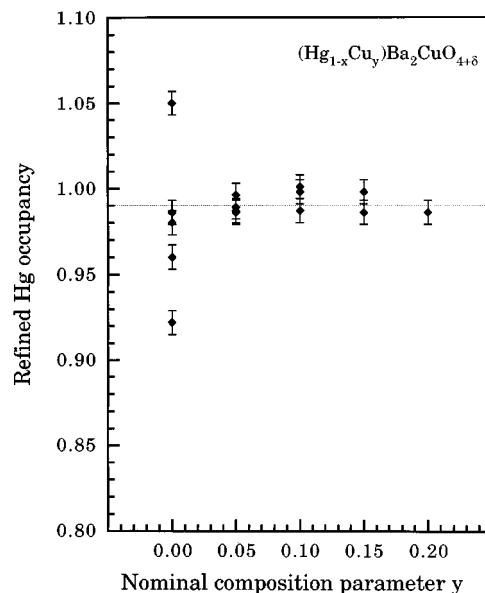


FIG. 9. Refined occupancies of the Hg site plotted against y , the amount of partial Cu substitution attempted.

($B_{\text{iso}} \sim 1.3 \text{ \AA}^2$) in all the refinements. Local distortions arising from the presence of an oxygen atom at the O(3) site may, by causing a certain amount of static displacement of Hg and O(2) off their respective sites, be responsible for the high thermal parameters observed.

F. Synthesis of monophasic Hg1201

Rietveld analysis of powder x-ray-diffraction data has shown that for these samples Cu does not partially substitute for Hg in the Hg1201 phase. It has also been demonstrated that the synthesis of Hg1201 from a reaction mixture of nominal composition $\text{HgBa}_2\text{CuO}_{4+\delta}$ normally leads to an impure product. However, monophasic Hg1201 can be synthesized using Hg-deficient reaction mixtures of nominal composition $\text{Hg}_{1-x}\text{Ba}_2\text{CuO}_{4+\delta}$ ($x=0.10$ for highest purity). Indeed, a recent article by Xue *et al.*²⁵ have reported similar findings. The final profile fit obtained from sample Hg(20), of nominal starting composition $\text{Hg}_{0.9}\text{Ba}_2\text{CuO}_{4+\delta}$ is presented in Fig. 10, and Table II lists the final refined structural and residual factors.

The use of a Hg-deficient reaction mixture to synthesize Hg1201 is both simple and highly reproducible. An explanation for this observation may be obtained from a recent publication by Zhou *et al.*²⁶ These authors performed a detailed high-resolution electron microscopy study on monophasic

TABLE III. The thermal parameters of Hg, Ba, Cu, O(1), and O(2) averaged over all the Rietveld refinements.

Atom	$B_{\text{iso}} (\text{\AA}^2)$
Hg	2.4(1)
Ba	1.7(1)
Cu	1.3(1)
O(1)	1.2(3)
O(2)	2.0(3)

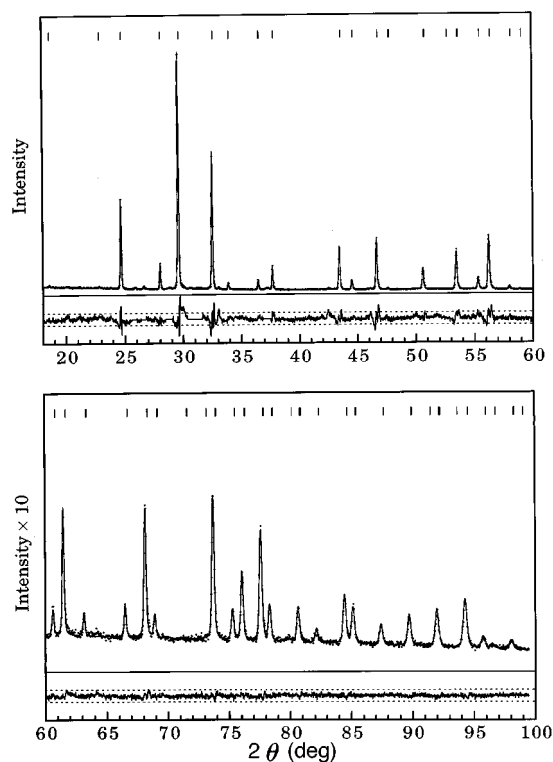


FIG. 10. The final profile fit for sample Hg(20), of nominal starting composition $\text{Hg}_{0.9}\text{Ba}_2\text{CuO}_{4+\delta}$. The difference/esd profile is displayed below the main profile, the dashed lines signifies ± 3 esd.

Hg1201 and revealed its complex surface chemistry. The surface of the Hg1201 grains were shown to consist of a coating of amorphous Ba_2CuO_3 , between 20 and 40 Å thick. Considering the thickness of this surface layer, the small size of the grains (2–10 μm) and the correspondingly large overall surface area, it would appear that this is the fate of the ~10% excess of $\text{Ba}_2\text{CuO}_{3.3}$ used in the synthesis of monophase Hg1201.

IV. CONCLUDING REMARKS

In conclusion, we have attempted the synthesis of $(\text{Hg}_{1-x}\text{Cu}_y)\text{Ba}_2\text{CuO}_{4+\delta}$ ($0 \leq x \leq 0.2$, $0 \leq y \leq 0.2$, $y \leq x$). However, a detailed Rietveld refinement analysis of powder x-ray-diffraction data collected on all 15 samples found no partial occupancy of the Hg site by Cu, i.e., in all cases the superconducting phase formed was simply $\text{HgBa}_2\text{CuO}_{4+\delta}$. We therefore conclude that no solid solution of the form $(\text{Hg}_{1-x}\text{Cu}_y)\text{Ba}_2\text{CuO}_{4+\delta}$ including the special case of $(\text{Hg}_{1-y}\text{Cu}_y)\text{Ba}_2\text{CuO}_{4+\delta}$ exists for these samples. Our findings are in agreement with a recently published article by Xiong *et al.*²⁷ These authors have investigated the synthesis of $\text{HgBa}_2\text{CuO}_{4+\delta}$ using Hg-deficient reaction mixtures and by a combination of powder x-ray and neutron-diffraction studies have determined that no significant partial substitution of Hg by Cu occurs within this system. Furthermore, our results suggest that phase pure $\text{HgBa}_2\text{CuO}_{4+\delta}$ can be synthesized from a Hg-deficient reaction pellet of nominal composition $\text{Hg}_{0.9}\text{Ba}_2\text{CuO}_{4+\delta}$. This is based on powder x-ray-diffraction results reported here and electron microscopy observations²⁶ which show the individual grains of $\text{HgBa}_2\text{CuO}_{4+\delta}$ to be coated with an amount of $\text{Ba}_2\text{CuO}_{3.3}$.

Only one interstitial oxygen site O(3) was determined in $\text{HgBa}_2\text{CuO}_{4+\delta}$ located exactly at the center of the Hg plane; no evidence was found for any displacement disorder of this site. This, together with the absence of any Cu substitution onto the Hg site, differs significantly from recent neutron-diffraction studies on the homologous series $\text{HgBa}_2\text{Ca}_{n-1}\text{Cu}_n\text{O}_{2n+n+\delta}$.^{4,9,11}

Detailed analysis of the structural refinements has produced a number of correlations between the exact location of Ba^{2+} cation within the unit-cell and critical superconducting parameters. These include the extent of the oxidation of the CuO_2 planes, the occupancy of the O(3) site, and the magnetic penetration depth.

ACKNOWLEDGMENTS

We thank EPSRC and The Royal Society for the financial support of this work.

* Author to whom correspondence should be addressed: Professor P. P. Edwards, School of Chemistry, The University of Birmingham, Birmingham B15 2TT, United Kingdom.

¹S. N. Putilin, I. Bryntse, and E. V. Antipov, *Mater. Res. Bull.* **26**, 1299 (1991).

²S. N. Putilin, E. V. Antipov, O. Chmaissem, and M. Marezio, *Nature (London)* **362**, 226 (1993).

³A. Schilling, M. Cantoni, J. D. Guo, and H. R. Ott, *Nature (London)* **363**, 56 (1993).

⁴J. L. Wagner, P. G. Radaelli, D. G. Hinks, J. D. Jorgensen, J. F. Mitchell, B. Dabrowski, G. S. Knapp, and M. A. Beno, *Physica C* **210**, 447 (1993).

⁵O. Chmaissem, Q. Huang, S. N. Putilin, M. Marezio, and A. Santoro, *Physica C* **212**, 307 (1993).

⁶S. M. Loureiro, E. V. Antipov, J. L. Tholence, J. J. Capponi, O. Chmaissem, Q. Huang, and M. Marezio, *Physica C* **217**, 253 (1993).

⁷Q. Huang, J. W. Lynn, R. L. Meng, and C. W. Chu, *Physica C* **218**, 356 (1993).

⁸O. Chmaissem, Q. Huang, E. V. Antipov, S. N. Putilin, M.

Marezio, S. M. Loureiro, J. J. Capponi, J. L. Tholence, and A. Santoro, *Physica C* **217**, 265 (1993).

⁹A. Asab, A. R. Armstrong, I. Gameson, and P. P. Edwards, *Physica C* **255**, 180 (1995).

¹⁰L. W. Finger, R. M. Hazen, R. T. Downs, R. L. Meng, and C. W. Chu, *Physica C* **226**, 216 (1994).

¹¹J. L. Wagner, B. A. Hunter, D. G. Hinks, and J. D. Jorgensen, *Phys. Rev. B* **51**, 15 407 (1995).

¹²H. M. Rietveld, *Acta Crystallogr.* **22**, 151 (1967).

¹³A. C. Larson and R. B. Von Dreele, LAUR 86748, Los Alamos National Laboratory (1987).

¹⁴A. M. Campbell, F. J. Blunt, J. D. Johnson, and P. A. Freeman, *Cryogenics* **31**, 732 (1991).

¹⁵J. R. Waldram, A. Porch, and H. M. Cheah, *Physica C* **232**, 189 (1994).

¹⁶V. A. Alyoshin, D. A. Mikhailova, and E. V. Antipov, *Physica C* **255**, 173 (1995).

¹⁷D. J. Singh, *Physica C* **212**, 228 (1993).

¹⁸Q. Xiong, Y. Y. Xue, Y. Cao, F. Chen, J. Gibson, L. M. Liu, A. Jacobson, and C. W. Chu, *Physica C* **251**, 216 (1995).

- ¹⁹M. R. Presland, J. L. Tallon, R. G. Buckley, R. S. Liu, and N. E. Flower, *Physica C* **176**, 95 (1991).
- ²⁰Q. Xiong, Y. Y. Xue, Y. Cao, F. Chen, Y. Y. Sun, J. Gibson, C. W. Chu, L. M. Liu, and A. Jacobson, *Phys. Rev. B* **50**, 10 346 (1994).
- ²¹I. D. Brown, *J. Solid State Chem.* **82**, 2322 (1989).
- ²²Y. J. Uemura, A. Keren, L. P. Le, Q. M. Luke, W. D. Wu, Y. Kubo, T. Maneko, Y. Shimakawa, M. Subramanian, J. L. Cobb, and J. T. Markett, *Nature (London)* **364**, 605 (1993).
- ²³C. Niedermayer, C. Bernhard, U. Binniger, H. Glückler, J. L. Tallon, E. J. Ansaldo, and J. I. Budnick, *Phys. Rev. Lett.* **71**, 1764 (1993).
- ²⁴S. M. Loureiro, E. T. Alexandre, E. V. Antipov, J. J. Capponi, S. de Brion, B. Souletie, J. L. Tholence, M. Marezio, Q. Huang, and A. Santoro, *Physica C* **243**, 1 (1995).
- ²⁵Y. Y. Xue, Q. Xiong, Y. Cao, I. Rusakova, Y. Y. Sun, and C. W. Chu, *Physica C* **255**, 1 (1995).
- ²⁶W. Zhou, A. Asab, I. Gameson, D. A. Jefferson, and P. P. Edwards, *Physica C* **248**, 1 (1995).
- ²⁷Q. Xiong, F. T. Chan, Y. Y. Xue, and C. W. Chu, *Physica C* **253**, 329 (1995).